ELSEVIER

Nuclear Engineering and Design 197 (2000) 75–87

Nuclear Engineering and Design

www.elsevier.com/locate/nucengdes

Elastic-plastic analysis of small cracks in tubes under internal pressure and bending

Jacob Foxen [a], Sharif Rahman [b,*,1]

[a] *John Deere Dubuque Works, 18600 S. John Deere Road, Dubuque, IA 52001, USA*
[b] *Department of Mechanical Engineering, The University of Iowa, 2140 Seamans Center, Iowa City, IA 52242, USA*

Received 28 January 1999; received in revised form 23 August 1999; accepted 13 September 1999

Abstract

Elastic-plastic finite element analyses were conducted to generate new solutions of *J*-integral and crack-opening displacement (COD) for short through-wall cracks in pipes subjected to combined bending and tension loads. The results are presented in terms of the well-known GE/EPRI influence functions to allow comparisons with some limited results in the literature. Two different pipe pressures with values of 7.24 MPa (1050 psi) and 15.51 MPa (2250 psi) simulating BWR and PWR operating conditions, respectively, were used to evaluate the effects of pressure on *J* and COD. Pipes with various radius-to-thickness ratios, crack sizes, and material parameters were analyzed. Limited analyses were also performed to evaluate the effects of hoop stresses in pipes under pure pressure loads. The results suggest that the fracture response parameters can be significantly increased by pressure-induced axial tension for larger crack size, material hardening constant, and radius-to-thickness ratio of the pipe. The presence of pressure-induced hoop stresses also increases the fracture response, but in low-hardening materials their effects are insignificant due to small plastic-zone size that was expected for the intensity of pipe pressure and crack size considered in this study. However, for high-hardening materials when the plastic-zone size is not negligible, the hoop stresses can moderately increase *J* and COD.

1. Introduction

Analytical methods for elastic-plastic fracture analysis of circumferential through-wall-cracked (TWC) pipes subjected to pure bending, pure tension, and combined bending and tension are well-developed. Brust et al. (1995a) and Rahman et al. (1995a, 1998a,b) have summarized several methods for predicting the *J*-integral and crack-opening displacement (COD) which are the most viable fracture parameters used to characterize nonlinear fracture behavior of cracked pipes. These methods consist of formulating analytical expressions for *J* and COD under various loading conditions. Classical *J*-tearing theory is utilized to evaluate the pipe's load-carrying capacity. Although, most of these methods are suitable for analyzing cracks in homogeneous materials (e.g. cracks in a base metal of the pipe), a method has

* Corresponding author. Tel.: +1-319-335-5679; fax: +1-319-335-5669.
E-mail address: rahman@icaen.uiowa.edu (S. Rahman)
[1] http://www.icaen.uiowa.edu/ ~ rahman

0029-5493/00/$ - see front matter
PII: S0029-5493(99)00258-7

also been recently developed to estimate J and COD for a through-wall crack in a pipe weld (Rahman and Brust, 1992a,b; Rahman et al., 1996).

During the recently completed United States Nuclear Regulatory Commission's Short Cracks in Piping and Piping Welds Program (Wilkowski et al., 1991–1995), the currently available analytical methods were evaluated by extensive comparisons with the experimental data. Two major technical reports, published by Brust et al., (1995a) and Rahman et al., (1995a), describe these methods and associated results involving various pipe geometries, crack sizes, and material properties. However, the ability of these estimation methods to predict fracture response and crack growth behavior for small cracks (crack length ≤ 12 % of pipe circumference) under combined bending and pressure loads has not been established, even though combined loading condition and small cracks are often a major concern for leak-before-break analysis and in-service flaw evaluation of large-diameter pipes in the nuclear power industry. Currently, a limited amount of finite element solutions are available for combined bending and tension loads. They were compiled only for an internal pressure of 15.51 MPa (2250 psi) simulating pressure condition in a piping system of pressurized water reactor (PWR) plants (Brust et al., 1995a; Rahman et al., 1995a). No such solutions currently exist for boiling water reactor (BWR) piping systems that has an internal pressure of 7.24 MPa (1050 psi) or any other magnitudes of pressure.

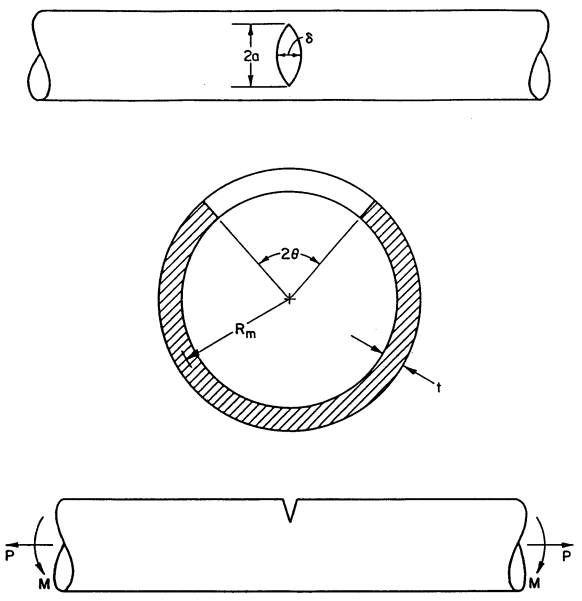

Fig. 1. A circumferentially through-wall-cracked pipe under combined bending and tension.

This paper presents new results from a series of elastic-plastic finite element analysis (FEA) for TWC pipes under combined bending and tension loads. The analyses were primarily based on the deformation theory of plasticity. A limited number of analyses were also performed using the incremental theory of plasticity to determine if the deformation theory produces adequate results. The analyses involved small cracks with various pipe geometries and material properties. The results were compiled as plastic influence functions for J-integral and COD in the spirit of GE/EPRI estimation method (Kumar and German, 1988). The effects of pressure on J and COD were evaluated due mainly to pressure-induced tensile load in an end-capped pipe. A limited amount of calculations were also made to study the effects of pressure-induced hoop stresses on J and COD. Typically, hoop stresses are neglected for calculating J and COD. This study attempts to quantify the effects of hoop stresses in pipe fracture analysis of small cracks.

2. A cracked pipe under combined bending and pressure

Consider a through-wall-cracked pipe with mean radius, R_m, wall thickness, t, and crack angle, 2θ, as shown in Fig. 1. The pipe is subjected to combined bending moment, M and axial tension force, P due to internal pipe pressure, p. For an end-capped pipe, $P = \pi R_i^2 p$, where R_i is the inside radius of the pipe. Typically, only this pressure-induced axial tension is considered in pipe fracture analysis (Kumar and German, 1988; Wilkowski et al., 1991–1995; Rahman and Brust, 1992a,b; Brust et al., 1995a; Rahman et al., 1995a, 1996, 1998a,b). It is assumed that the constitutive

law characterizing the material's stress-strain ($\sigma - \varepsilon$) response can be represented by the well-known Ramberg–Osgood model

$$\frac{\varepsilon}{\varepsilon_0} = \frac{\sigma}{\sigma_0} + \alpha\left(\frac{\sigma}{\sigma_0}\right)^n \tag{1}$$

in which σ_0 is the reference stress which can be arbitrary, but is usually assumed to be the yield stress, E is the modulus of elasticity, $\varepsilon_0 = \sigma_0/E$ is the associated reference strain, and α and n are the model parameters usually chosen from best fit of actual laboratory data.

For circumferential TWC pipes, elastic-plastic analysis techniques, which do not require full three-dimensional FEA for combined bending and tension loads, are scarce. Paris and Tada (1983) have presented a method, which interpolates between the known elastic and rigid-plastic solutions by using a pseudo plastic-zone correction to the elastic solution. Klecker et al. (1986) introduced a method, which is very similar to the Paris and Tada (1983) approach, except it accounts for material strain hardening empirically. Both of these methods require numerical integration. Recently, Kumar and German (1988) presented a method, which is based upon interpolation between compiled finite-element solutions. The British R6 method (Milne et al., 1988) was developed to predict failure loads for pipes subjected to combined bending and tension. However, displacements were not provided. It should be noted that methods for the purely elastic problem have been available for some time now as summarized by Forman et al. (1985).

The discussions on the conditions for achieving J-dominance and the suitability of J as a fracture parameter for combined bending and tensile loading have been presented by Shih (1985) and Shih and Hutchinson (1986) by studying the single-edge-notched tension (SENT) specimen. Additional studies based on FEA of the SENT specimens subjected to combined tension and bending have also appeared (Kaiser, 1985; Sönnerlind and Kaiser, 1986). An important result obtained by Sönnerlind and Kaiser (1986) indicates that the value of J is essentially independent of whether tension is applied, then bending; bending then tension; or both tension and bending are applied proportionally. This is not intuitively obvious since such loading clearly violates the hypothesis (necessary for valid J-tearing theory) of proportional loading. Based on this premise, a deterministic equivalence method using reduced section analogy of a cracked pipe was proposed by Brust and Gilles (1994) for evaluating J under combined bending and tension loads. Later, Rahman et al. (1993a,b, 1995b) and Wilkowski et al. (1993) extended this method to include stochastic treatment of fracture-mechanics variables for probabilistic pipe fracture evaluations.

3. The GE/EPRI estimation method for combined loading

The GE/EPRI method is based on a compilation of limited finite element solutions for TWC pipes using the deformation theory of plasticity. From the deformation theory of plasticity, the fracture response parameters, such as J and center-crack-opening displacement, δ, can be split into elastic and plastic components, as

$$J = J_e + J_p \tag{2}$$

$$\delta = \delta_e + \delta_p \tag{3}$$

where the subscripts 'e' and 'p' refer to the elastic and plastic contributions, respectively. Each component of the fracture parameters above can be expressed in terms of dimensionless influence functions that depend on normalized pipe geometry (R_m/t), normalized crack size (θ/π), material hardening constant (n), and loading condition. Under combined bending and tension loads, J_e and δ_e can be expressed via linear combinations of stress-intensity factor (K_I) and COD due to pure bending (K_I^B, δ_e^B) and pure tension (K_I^T, δ_e^B) loads applied separately (Kumar and German, 1988; Wilkowski et al., 1991–1995; Rahman and Brust, 1992a,b; Brust et al., 1995a; Rahman et al., 1995a, 1996, 1998a,b), i.e.

$$J_e = \frac{(K_I^B + K_I^T)^2}{E} \tag{4}$$

$$\delta_e = \delta_e^B + \delta_e^T \tag{5}$$

where

$$K_I^B = \frac{MR_m}{I}\sqrt{\pi a}\ F_B(\theta/\pi, R_m/t), \tag{6}$$

$$K_I^T = \frac{P}{2R_m t}\sqrt{\frac{a}{\pi}}\ F_T(\theta/\pi, R_m/t), \tag{7}$$

$$\delta_e^B = 4a\frac{R_m}{I}V_1^B(\theta/\pi, R_m/t)\frac{M}{E}, \tag{8}$$

$$\delta_e^T = \frac{2a}{\pi R_m t}V_1^T(\theta/\pi, R_m/t)\frac{P}{E} \tag{9}$$

$a = R_m\theta$ is the half crack length at mean pipe diameter, $I \cong \pi R_m^3 t$ is the moment of inertia (for large R_m/t) of uncracked pipe cross-section about its centroidal axis, $F_B(\theta/\pi, R_m/t)$ and $F_T(\theta/\pi, R_m/t)$ are elastic influence functions for J-integral under pure bending and pure tension loads, respectively, and $V_1^B(\theta/\pi, R_m/t)$ and $V_1^T(\theta/\pi, R_m/t)$ are elastic influence functions for center-crack-opening displacement under pure bending and pure tension loads, respectively. The superposition principle invoked in Eqs. (4) and (5) is valid due to linear-elastic stress analysis. For plastic J and δ, however, there are several approaches in introducing the plastic influence functions.

3.1. Approach 1

In the first approach, a dimensionless load factor $\lambda = M/PR_m$ can be used to define a proportionality relationship between tension force, P and moment, M. Accordingly (Kumar and German, 1988),

$$J_p = \alpha\sigma_0\varepsilon_0 a\left(1-\frac{\theta}{\pi}\right)h_1^{B+T}(\theta/\pi, n, R_m/t, \lambda)\left(\frac{P}{P_0'}\right)^{n+1} \tag{10}$$

$$\delta_p = \alpha\varepsilon_0 a h_2^{B+T}(\theta/\pi, n, R_m/t, \lambda)\left(\frac{P}{P_0'}\right)^{n} \tag{11}$$

where $h_1^{B+T}(\theta/\pi, n, R_m/t, \lambda)$ and $h_2^{B+T}(\theta/\pi, n, R_m/t, \lambda)$ are plastic influence functions for J and δ, respectively, under combined bending and tension loads,

$$M_0 = 4\sigma_0 R_m^2 t\left[\cos\frac{\theta}{2} - \frac{1}{2}\sin\theta\right], \tag{12}$$

$$P_0 = 2\sigma_0 R_m t\left[\pi - \theta - 2\sin^{-1}\left(\frac{1}{2}\sin\theta\right)\right], \tag{13}$$

and

$$P_0' = \frac{1}{2}\left[-\frac{\lambda P_0^2 R_m}{M_0} + \sqrt{\left(\frac{\lambda P_0^2 R_m}{M_0}\right)^2 + 4P_0^2}\right] \tag{14}$$

The expressions for reference loads M_0, P_0, and P_0' in Eqs. (12)–(14) are identical to those for the corresponding limit loads of a TWC pipe under pure bending, pure tension, and combined bending and tension, respectively, if σ_0 is replaced by the collapse of flow stress of the material. Note that the GE/EPRI plastic functions h_1 and h_2 are now also functions of λ. This approach, although theoretically rigorous, is not very convenient for pipes subjected to a fixed internal pressure and varying bending moment, which is the case in nuclear piping for BWR and PWR systems. Due to the addition of one more variable (λ), the number of variables h_1 or h_2 is a function of, increases from three to four. Consequently, the matrix of finite element calculations for determining these h-functions can become enormously large. Nevertheless, some limited solutions of h-functions using λ were compiled by Kishida and Zahoor (1988).

3.2. Approach 2

In the second approach, it is proposed that the plastic h-functions be evaluated for a fixed internal pressure and increasing bending moment using procedures similar to those used for tension and bending alone. For example, the calculated h values can be determined for an internal pressure of 15.51 MPa (2250 psi) and 7.24 MPa (1050 psi) simulating operating conditions at PWR and BWR plants, respectively. This is the approach undertaken by the authors to conduct new finite element calculations of the h-functions in this paper. In this approach,

$$J_p = \alpha\sigma_0\varepsilon_0 a\left(1-\frac{\theta}{\pi}\right)h_1^T(\theta/\pi, n, R_m/t)\left(\frac{P}{P_0}\right)^{n+1} + \alpha\sigma_0\varepsilon_0 a\left(1-\frac{\theta}{\pi}\right)h_1^{B+T}(\theta/\pi, n, R_m/t)\left(\frac{M}{M_0}\right)^{n+1} \tag{15}$$

$$\delta_p = \alpha\varepsilon_0 a h_2^T(\theta/\pi, n, R_m/t)\left(\frac{P}{P_0}\right)^{n} + \alpha\varepsilon_0 a h_2^{B+T}(\theta/\pi, n, R_m/t)\left(\frac{M}{M_0}\right)^{n} \tag{16}$$

where $h_1^{\mathrm{T}}(\theta/\pi, n, R_m/t)$ and $h_2^{T}(\theta/\pi, n, R_m/t)$ are plastic influence functions for J and δ, respectively, under pure tension, and $h_1^{\mathrm{B+T}}(\theta/\pi, n, R_m/t)$ and $h_2^{\mathrm{B+T}}(\theta/\pi, n, R_m/t)$ are plastic influence functions for J and δ, respectively, under bending in the presence of a fixed tension load. The first term in the right hand side of Eqs. (15) and (16) represents plastic contributions of fracture parameters under tensile load before the application of bending moment. By no means, Eqs. (15) and (16) represent linear superposition, since $h_1^{\mathrm{B+T}}$ and $h_2^{\mathrm{B+T}}$ functions always include the effects of tension under combined bending and tension loads. Past work of Brust et al. (1995a) involved calculations of $h_1^{\mathrm{B+T}}$ and $h_2^{\mathrm{B+T}}$ using Eqs. (15) and (16), but only the results for the PWR pressure condition ($p = 15.51$ MPa [2250 psi]) were reported. No similar calculations were done for the BWR pressure condition ($p = 7.24$ MPa [1050 psi]) or any other pressures. Developing solutions of h-functions for BWR pressure condition is one of the motivations of the present study. It should be noted that h-functions for pure bending problem (i.e. $p = 0$) have also been developed by Brust et al. (1995b).

4. Finite element simulation

4.1. Deformation and flow theories of plasticity

In defining the constitutive equations for nonlinear finite element analysis of work-hardening materials, there are two major plasticity theories that can be used to calculate the GE/EPRI functions $h_1^{\mathrm{B+T}}$ and $h_2^{\mathrm{B+T}}$ in Eqs. (15) and (16). The first type of formulation is the deformation theory in the form of total stress-strain relationship (Kachanov, 1974). This theory assumes that the state of stress determines the state of strain uniquely as long as the plastic deformation continues. This is identical to the nonlinear elastic stress-strain relationship with no unloading and is valid for loading paths that are only proportional. The second type of formulation is the incremental or flow theory in the form of the incremental stress-strain relationship. This theory relates the increment of plastic strain components to the state of stress and the stress increment. It is more general than the deformation theory and can be applied for a wide variety of loading conditions including nonproportional and cyclic loads (Kachanov, 1974). For a typical monotonic pipe test under combined bending and tension, the tensile force is usually held constant due to constant internal pressure, but the bending moment is gradually increased until the maximum-load carrying capacity of the pipe is reached. During the progression of load increments, the load factor, λ, which is defined as the nondimensionalized ratio of bending moment and tension, also increases, thus violating load proportionality, the essential condition to the validity of deformation theory of plasticity. However, this nonproportionality caused by applying tension first, followed by bending, or vice-versa, has little effect on both the path independence of J and on the final value of J at the end of the complete loading. In other words, for practical purposes, it is not important whether tension is applied first, followed by bending, bending followed by tension, or both tension and bending are applied simultaneously. Sönnerlind and Kaiser (1986) have shown this by investigating the two-dimensional SENT specimens subjected to combined bending and tension. The authors will show this here for the three-dimensional TWC pipe problem involving combined bending and tension loads.

In addition, the typical values of service pressure in a pipe are 15.51 MPa (2250 psi) for PWR and 7.24 MPa (1050 psi) for BWR. The pipe material behavior under these pressure loading alone is mostly elastic with a small plastic zone for the crack sizes considered here. Hence, both deformation and flow theories should be equally applicable for finite element analysis to determine the GE/EPRI influence functions.

4.2. Validation of deformation theory

In order to substantiate that the deformation theory produces adequate results for nonproportional loading, a verification study was conducted. As an example, consider a TWC pipe with $R_m/t = 10$, $n = 5$, and $\theta/\pi = 1/8$, which is subjected to axial tension corresponding to an internal pres-

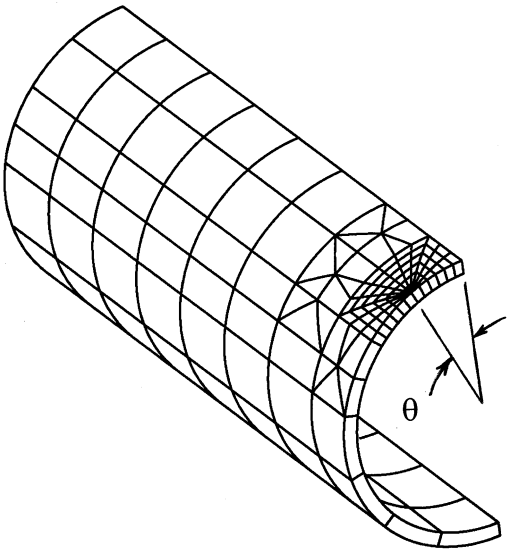

Fig. 2. A finite element mesh with $R_m/t = 10$ and $\theta/\pi = 1/8$ (1/4 model).

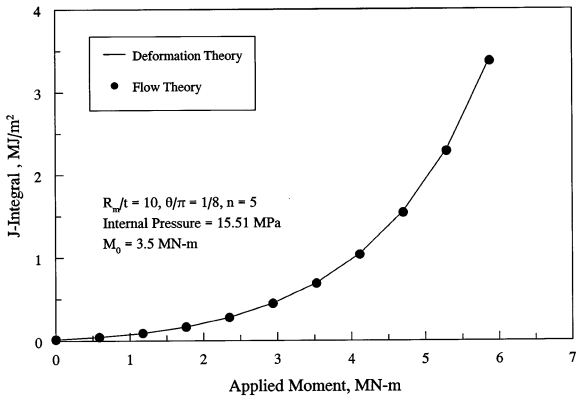

Fig. 3. J-integral calculations by deformation and flow theories for non-proportional loading.

sure of 15.51 MPa (2250 psi) and bending moment of increasing magnitudes. It is assumed that the material's stress-strain relationship can be represented by the Ramberg–Osgood equation defined by Eq. (1). Two finite element analyses were carried out for this pipe using deformation and incremental stress-strain formulations. The computer code used was ABAQUS (ABAQUS, 1996) with twenty-noded, three-dimensional isoparametric solid elements. A finite element mesh for a quarter model of the pipe is shown in Fig. 2. In both analyses, the axial tension due to the pressure was applied first, followed by the application of bending moment. During the application of moment, the tension force was held constant.

As shown in Fig. 2, only one element is used in the radial direction. A mesh refinement study, performed by Firmature (1998) and Firmature and Rahman (1999), showed that the difference in the values of thickness-averaged J from finite element analyses based on one-element and two-element models is $< 2\%$. Hence, finite element meshes with one element through the thickness of the pipe were used to reduce the computational effort for all analyses conducted in this study. Furthermore, a weighted-average of local J-values calculated at inside (J_1), middle (J_2), and outside (J_3) crack-tips, which is given by

$$J = \frac{J_1 + 4J_2 + J_3}{6} \tag{17}$$

was used for all J calculations presented in this paper. The local variations of J were not explored in this study.

Fig. 3 shows the results of both analyses presented in terms of J-integral plots as a function of applied bending moment. They clearly indicate that the finite element results by deformation theory provide accurate estimates of crack driving force when compared with those obtained from flow or incremental theory. Fig. 4 shows the percentage error for various applied moments,

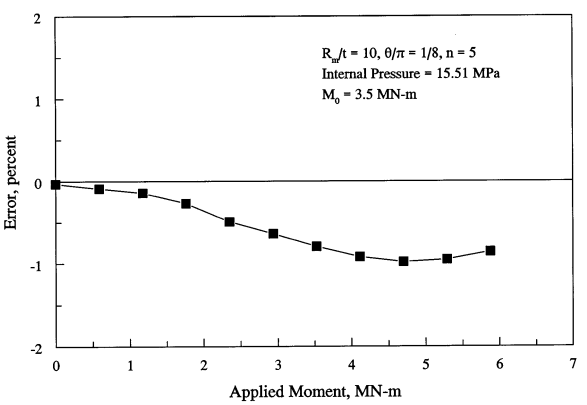

Fig. 4. Error in J-integral by deformation theory of plasticity for non-proportional loading.

Table 1
Matrix of finite element calculations for short through-wall-cracked pipes under combined bending and tension (total of 30 analyses)

Model no.	Model name	R_m/t	n	θ/π	Remarks	Loading
1	CASE1A3DTMBWR	5	2,3,5,7,10	0.0625	5 Runs	Tension and bending
2	CASE2A3DTMBWR	10	2,3,5,7,10	0.0625	5 Runs	Tension and bending
3	CASE3A3DTMBWR	20	2,3,5,7,10	0.0625	5 Runs	Tension and bending
4	CASE1B3DTMBWR	5	2,3,5,7,10	0.1250	5 Runs	Tension and bending
5	CASE2B3DTMBWR	10	2,3,5,7,10	0.1250	5 Runs	Tension and bending
6	CASE3B3DTMBWR	20	2,3,5,7,10	0.1250	5 Runs	Tension and bending

where the error is defined as the ratio of the difference between J from flow theory and deformation theory to J from flow theory $\times 100$. From this figure, it appears that the prediction based on deformation theory is slightly higher than that based on flow theory. But, the maximum absolute error is $< 1\%$. Hence, the deformation theory was adequate for use in the rest of the finite element analyses. This allowed significant savings of computational effort in determining the GE/EPRI functions and results in a simpler estimation scheme. In the original GE/EPRI method for combined bending and tension (Kumar and German, 1988), a λ factor was defined (i.e. Approach 1). The h-functions were compiled for some limited values of λ. Since the axial tension in a nuclear piping system is constant and the bending moment is constantly increased, λ changes throughout the analysis. This makes the GE/EPRI analysis inconvenient since as λ changes during the moment application phase, the h-functions change, and one must re-interpolate throughout the tables of h-functions. With the proposed approach (i.e. Approach 2) in this study, the h-functions are constant as long as the pipe geometry, crack size, material properties, and axial tension remain unchanged. All of the h-functions calculated and presented in this study are based on this second approach.

4.3. Finite element model and analysis matrix

Following validation of deformation theory, six finite element meshes were developed, one for each case listed in Table 1. They involved pipes with a constant mean radius, $R_m = 355.6$ mm (14 inches) and a variable thickness, $t = 71.12$ mm (2.8 inches), 35.56 mm (1.4 inches), and 17.78 mm (0.7 inch) to model three pipes with $R_m/t = 5$, 10, and 20, respectively. For each of these three pipes, crack sizes with $\theta/\pi = 1/16$ and $1/8$ (i.e. small cracks) were considered. A typical finite element mesh with $R_m/t = 10$ and $\theta/\pi = 1/8$ is illustrated in Fig. 2. A quarter model was used to take advantage of symmetry. Twenty-noded isoparametric brick elements were used with focused elements at the crack tip. In the crack-tip region, a ring of 12 wedge-shaped elements was used. These wedge-shaped elements were constructed by collapsing the appropriate nodes of twenty-noded solid elements to produce $1/r$ strain singularity. Although, this type of singularity is strictly valid for a fully plastic crack-tip field of non-hardening materials ($n \to \infty$), it is practically adequate for work-hardening materials with sufficiently refined crack-tip mesh. For the material properties, the following values were used: $E = 207$ GPa (30,000 ksi), $\nu = 0.4$, and $\sigma_0 = 344.8$ MPa (50 ksi), $\alpha = 1$. These values, in addition to the values of $n =$ 2,3,5,7,9, should provide complete characterization of the pipe material properties according to Eq. (1). The applied bending moment varied according to the pipe and crack geometry studied. However, in all cases the applied moment was large enough so that the influence functions remain invariant with respect to further loading. Only one element through the pipe wall was used, and, as such, the tabulated results should be considered as average values through the pipe wall (see Eq. (17)).

The finite element analysis for each case was performed in two load steps. In the first step, an axial tension force corresponding to pipe internal pressure was applied to the end of the pipe. The

second step consists of increasing bending load until fully plastic conditions were met. The deformation theory of plasticity algorithm was used in both load steps. A reduced 2×2 Gaussian quadrature rule was used for numerical integration. All analyses were performed using the commercial finite element code ABAQUS (1996).

5. Results and discussions

5.1. Effects of axial tension

Tables 2–4 show the h_1- and h_2-functions for pipes that are subjected to combined bending and tension due to an internal pressure of $p = 7.24$ MPa (1050 psi) for $R_m/t = 5$, 10, and 20, respectively. They were calculated for small cracks, e.g. $\theta/\pi = 1/16$ and 1/8, and several values of material hardening constant, e.g. $n = 2$, 3, 5, 7, and 10. To evaluate the effects of tension on J and COD, these functions evaluated for $p = 15.51$ MPa (2250 psi) and $p = 0$ MPa (0 psi) [i.e. pure bending] from past studies (Brust et al., 1995a; Rahman et al., 1995a) are also presented in Tables 5–10.

Fig. 5 shows the effects of tension on h_1 as a function of n for several values of θ/π and R_m/t. The values of h_1 and hence J increase with pressure (p) regardless of n. The effect of pressure appears to be significant for thin-walled pipes and is clearly shown in the results for $R_m/t = 20$. This is, however, expected since the longitudinal tensile

Table 2
Tabulation of h-functions for short through-wall-cracked pipes under combined bending and tension[a]

Crack size	Function	$n = 2$	$n = 3$	$n = 5$	$n = 7$	$n = 10$
$\theta/\pi = 1/16$	h_1	5.279	5.606	5.893	5.897	5.288
	h_2	6.744	7.008	7.079	6.908	6.099
$\theta/\pi = 1/8$	h_1	4.677	4.578	4.126	3.654	2.739
	h_2	6.046	5.823	5.104	4.419	3.240

[a] For $R_m/t = 5$ ($p = 7.24$ MPa [1050 psi]).

Table 3
Tabulation of h-functions for short through-wall-cracked pipes under combined bending and tension[a]

Crack size	Function	$n = 2$	$n = 3$	$n = 5$	$n = 7$	$n = 10$
$\theta/\pi = 1/16$	h_1	5.740	6.208	6.936	7.305	6.870
	h_2	6.818	7.281	7.879	8.172	7.577
$\theta/\pi = 1/8$	h_1	5.858	5.916	5.744	5.118	4.578
	h_2	6.735	6.752	6.415	5.641	4.944

[a] For $R_m/t = 10$ ($p = 7.24$ MPa [1050 psi]).

Table 4
Tabulation of h-functions for short through-wall-cracked pipes under combined bending and tension[a]

Crack size	Function	$n = 2$	$n = 3$	$n = 5$	$n = 7$	$n = 10$
$\theta/\pi = 1/16$	h_1	6.481	7.170	8.999	10.162	10.321
	h_2	7.362	8.020	9.731	10.844	10.955
$\theta/\pi = 1/8$	h_1	8.297	8.564	8.988	9.332	8.103
	h_2	8.160	8.443	9.019	9.126	7.982

[a] For $R_m/t = 20$ ($p = 7.24$ MPa [1050 psi]).

Table 5
Tabulation of h-functions for short through-wall-cracked pipes combined bending and tension[a]

Crack size	Function	$n=2$	$n=3$	$n=5$	$n=7$	$n=10$
$\theta/\pi=1/16$	h_1	5.408	5.725	6.060	5.967	5.341
	h_2	6.851	7.115	7.232	6.979	6.153
$\theta/\pi=1/8$	h_1	4.837	4.682	4.338	3.996	3.064
	h_2	6.182	5.918	5.312	4.766	3.580

[a] For $R_m/t=5$ ($p=15.51$ MPa [2250 psi]).

Table 6
Tabulation of h-functions for short through-wall-cracked pipes under combined bending and tension[a]

Crack size	Function	$n=2$	$n=3$	$n=5$	$n=7$	$n=10$
$\theta/\pi=1/16$	h_1	5.929	6.409	7.157	8.052	8.312
	h_2	6.973	7.460	8.108	8.923	9.009
$\theta/\pi=1/8$	h_1	6.051	6.066	6.206	5.618	6.294
	h_2	6.888	6.868	6.844	6.181	6.578

[a] For $R_m/t=10$ ($p=15.51$ MPa [2250 psi]).

Table 7
Tabulation of h-functions for short through-wall-cracked pipes under combined bending and tension[a]

Crack size	Function	$n=2$	$n=3$	$n=5$	$n=7$	$n=10$
$\theta/\pi=1/16$	h_1	6.734	7.484	10.251	13.544	15.243
	h_2	7.561	8.292	10.924	14.078	15.813
$\theta/\pi=1/8$	h_1	8.621	8.917	10.846	13.282	13.836
	h_2	8.375	8.705	10.383	12.479	13.051

[a] For $R_m/t=20$ ($p=15.51$ MPa [2250 psi]).

Table 8
Tabulation of h-functions for short through-wall-cracked pipes under pure bending[a]

Crack size	Function	$n=2$	$n=3$	$n=5$	$n=7$	$n=10$
$\theta/\pi=1/16$	h_1	5.202	5.451	5.766	5.681	5.263
	h_2	6.686	6.896	7.003	6.715	6.087
$\theta/\pi=1/8$	h_1	4.575	4.484	3.976	3.372	2.464
	h_2	5.972	5.820	4.999	4.164	2.959

[a] For $R_m/t=5$ ($p=0$ MPa [0 psi]).

stress is inversely proportional to the pipe wall thickness for a given internal pressure.

Fig. 6 shows the similar evaluation of the effects of tension on h_2 and hence COD. The values of h_2 are slightly higher than those of h_1. As before, the effects of tension are more significant for larger R_m/t. Note that in these calculations, only the tension force due to the pipe pressure was included. No hoop stresses were modeled to be consistent with the past GE/EPRI solutions

(Brust et al., 1995a; Rahman et al., 1995a; Kumar and German, 1988).

5.2. Effects of hoop stress

In order to evaluate the effects of hoop stresses in a pipe, limited finite-element analyses were also conducted. The analyses were performed for a short crack using Model 2 (CASE2A3DTMBWR) in Table 1 with $R_m/t = 10$, $\theta/\pi = 1/16$, and $n = 2$, 5, 7, and 10. The effect of pressure was simulated by simultaneous applications of axial tension and internal pressure applied to all inside pipe elements. As a first step, only the pressure loading was considered without any bending moments.

Fig. 7 shows the ratio of the J-integral under combined tensile and hoop stresses (J^{T+H}) to the J-integral under axial tensile stress (J^T) as a function of internal pressure (p) for several values of n. The presence of hoop stress increases J and its effects on J also increases with the magnitude of pipe pressure as expected. However, this increase is insignificant for low-hardening materials (i.e. materials with larger n values). For example, the largest and smallest increases of J due to hoop stress are about 15% when $n = 2$ and 4% when $n = 10$, both when $p = 15.51$ MPa (2250 psi). This can be explained by the fact that when n is large, the plastic deformation around the crack-tip for such a small crack is small even when $p = 15.51$ MPa (2250 psi). Hence, the plastic contribution of J is very small. This can also be seen from the first term in the right hand side of Eq. (15) that indicates that J_p under pure tension decreases with n when $P < P_0$, which is the case for the magnitudes of pipe pressure used in these analyses. Except for $n = 2$ (high-hardening materials), Fig. 7 shows the effects of hoop stresses mostly on the elastic part of J and they are insignificant. Had the analyses been continued for higher pipe pressures or larger cracks to produce significant plastic deformation, J^{T+H}/J^T in Fig. 7 would have been much higher and the plots would have shown opposite trend for n when $P > P_0$. They were not explored in this study.

Fig. 8 shows the similar plots of the ratio of the COD under combined tensile and hoop stresses (δ^{T+H}) to the COD under axial tensile stress (δ^T) as a function of pressure (p) for several values of n. As before, the presence of hoop stresses increases COD only for large magnitudes of pressure and small values of n. When $p = 15.51$ MPa (2250 psi) and $n = 2$, the increase in COD is $\approx 13\%$. Similar to J, the effects of COD would

Table 9
Tabulation of h-functions for short through-wall-cracked pipes under pure bending[a]

Crack size	Function	$n = 2$	$n = 3$	$n = 5$	$n = 7$	$n = 10$
$\theta/\pi = 1/16$	h_1	5.588	6.225	6.761	6.784	6.749
	h_2	6.701	7.422	7.739	7.632	7.527
$\theta/\pi = 1/8$	h_1	5.694	5.791	5.512	4.790	3.823
	h_2	6.619	6.654	6.319	5.329	4.221

[a] For $R_m/t = 10$ ($p = 0$ MPa [0 psi]).

Table 10
Tabulation of h-functions for short through-wall-cracked pipes under pure bending[a]

Crack size	Function	$n = 2$	$n = 3$	$n = 5$	$n = 7$	$n = 10$
$\theta/\pi = 1/16$	h_1	6.272	7.044	8.022	8.756	8.815
	h_2	7.155	7.073	8.050	8.787	8.812
$\theta/\pi = 1/8$	h_1	8.019	8.448	8.281	7.748	6.524
	h_2	7.934	7.498	7.491	7.160	5.890

[a] For $R_m/t = 20$ ($p = 0$ MPa [0 psi]).

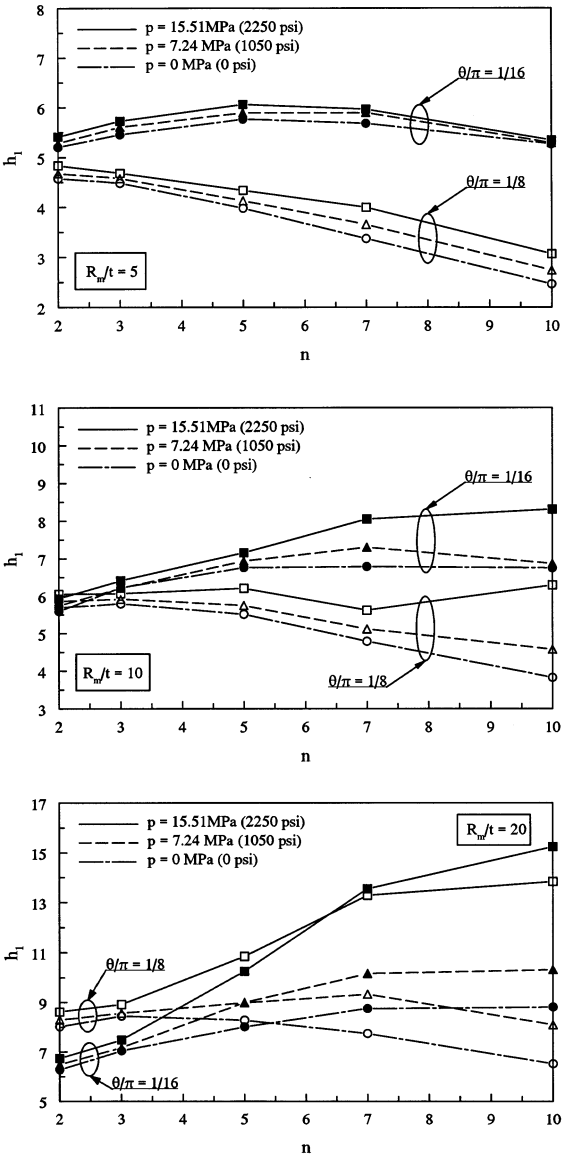

Fig. 5. Effects of pressure-induced axial tension on h_1 for small cracks.

have been much higher for larger cracks or much higher pipe pressures.

6. Summary and conclusions

Elastic-plastic finite element analyses were performed to generate new solutions of J-integral and crack-opening displacement for small cracks in pipes under combined bending and tension loads. First, the finite element results using the deformation theory of plasticity were validated against the results from the incremental theory of plasticity. Second, the finite element results were compiled as plastic influence functions for J and COD in the spirit of GE/EPRI estimation

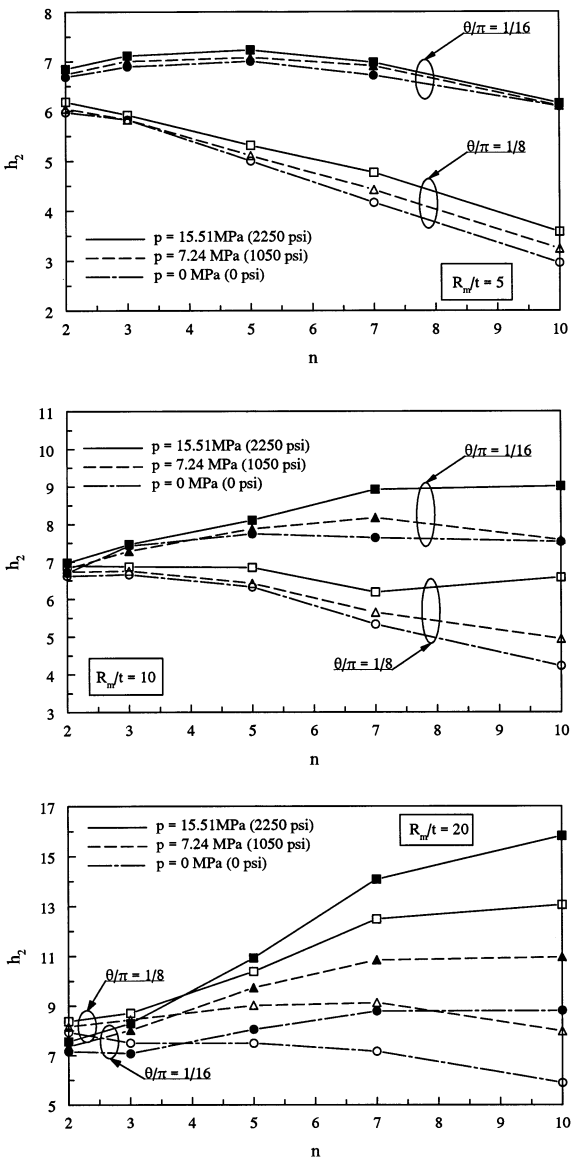

Fig. 6. Effects of pressure-induced axial tension on h_2 for small cracks.

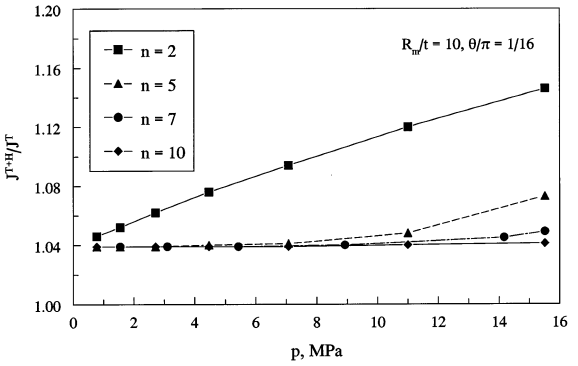

Fig. 7. Effects of hoop stress on J-integral for small cracks under pure pressure.

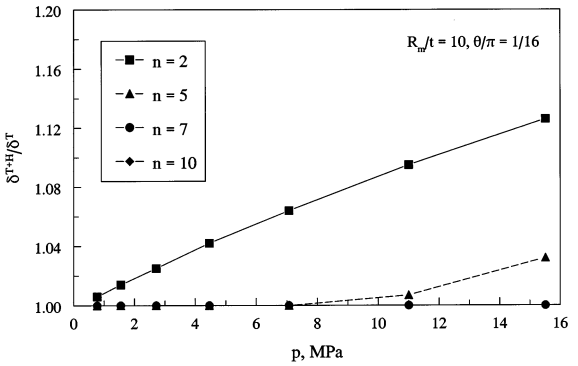

Fig. 8. Effects of hoop stress on COD for small cracks under pure pressure.

method. The new results will significantly enhance the current library of J and COD solutions. Limited finite element analyses were also performed to study the effects of pressure-induced hoop stresses on J and COD. The results showed that:

- The deformation theory of plasticity produces accurate results of J-integral for small cracks under combined bending and tension loads when compared with the results of the incremental theory of plasticity. Hence, the deformation theory can be used for calculating the GE/EPRI influence functions under combined loading.
- The axial tension in a pipe increases the values of h_1 (J-integral) and h_2 (COD) for pipes under combined bending and tension. The increase can be significantly large for pipes with larger crack size, material hardening constant, and radius-to-thickness ratio of the pipe. In particular, the axial tension can significantly increase both h_1 and h_2 for thin-walled pipe, because the tension load is inversely proportional to the pipe thickness.
- The presence of circumferential hoop stresses in a TWC pipe increases both J-integral and COD under pure pressure loading. In general, the effect of hoop stresses increases with the pipe pressure, but it is largely insignificant, except for high-hardening pipe materials with smaller values of n. This is mainly because of the small plastic-zone size for short cracks and pressure magnitudes considered in the analyses. However, for small values of n, when the plastic contribution of fracture parameters is not negligible, the hoop stresses may have moderate effects on J and COD. For a pipe with $R_m/t = 10$, $\theta/\pi = 1/16$, and $n = 2$, J and COD increased by 15 and 13%, respectively, under a pressure of 15.51 MPa (2250 psi), when the hoop stresses are included in the analyses.

Acknowledgements

Part of the work presented in this paper was supported by the Faculty Early Career Development Program of the United States National Science Foundation (Grant No. CMS-9833058). The program directors were Drs Sunil Saigal and Ken Chong.

References

ABAQUS, 1996. User's Guide and Theoretical Manual, Version 5.5. Hibbitt, Karlsson, & Sorensen, Pawtucket, RI.

Brust, F.W., Gilles, P., November 1994. Approximate methods for fracture analysis of tubular members subjected to combined tensile and bending loads. ASME J. Offshore Mech. Arctic Eng. 116, 221–227.

Brust, F.W., Scott, P., Rahman, S., Ghadiali, N., Kilinski, T., Francini, B., Marschall, C.W., Miura, N., Krishnaswamy, P., Wilkowski, G.M., April 1995. Assessment of Short Through-Wall Circumferential Cracks in Pipes-Experiments and Analysis, NUREG/CR-6235. U.S. Nuclear Regulatory Commission, Washington, DC.

Brust, F.W., Rahman, S., Ghadiali, N., 1995b. Elastic-plastic analysis of small cracks in tubes. J. Offshore Mech. Arctic Eng. 117, 57–62.

Firmature, R., Rahman, S., 1999. Elastic-plastic analysis of off-centered cracks in cylindrical structures. Submitted for publication.

Firmature, R., July 1998. Elastic-Plastic Analysis of Off-Centered Cracks in Cylindrical Structures, a thesis for Master of Science. Department of Mechanical Engineering, The University of Iowa, Iowa City, IA.

Forman, R.G., Hickman, J.C., Shivakumar, V., 1985. Stress intensity factors for circumferential through cracks in hollow cylinders subjected to combined tension and bending loads. Eng. Fract. Mech. 21 (3), 563–571.

Kachanov, L.M., 1974. Fundamentals of the Theory of Plasticity. MIR, Moscow.

Kaiser, S., 1985. An extension of tearing instability theory to multiple loading parameters. Int. J. Fract. 29, 85–99.

Kishida, K., Zahoor, A., August 1988. Crack-Opening Area Calculations for Circumferential Through-Wall Pipe Cracks, EPRI Special Report NP-5959-SR. Electric Power Research Institute, Palo Alto, CA.

Klecker, R., Brust, F., Wilkowski, G., May 1986. NRC Leak-Before-Break (LBB.NRC) Analysis Method for Circumferentially Through-Wall-Cracked Pipes Under Axial Plus Bending Loads, NUREG/CR-4572. U.S. Nuclear Regulatory Commission, Washington, DC.

Kumar, V., German, M., January 1988. Elastic-Plastic Fracture Analysis of Through-Wall and Surface Flaws in Cylinders, EPRI Topical Report, NP-5596. Electric Power Research Institute, Palo Alto, CA.

Milne, I., Ainsworth, R.A., Dowling, A.R., Stewart, A.T., 1988. Assessment of the integrity of structures containing defects. Int. J. Press. Vessels Pip. 32, 3–104.

Paris, P.C., Tada, H., September 1983. The Application of Fracture Proof Design Methods Using Tearing Instability Theory to Nuclear Piping Postulating Circumferential Through-Wall Cracks, NUREG/CR-3464. U.S. Nuclear Regulatory Commission, Washington, DC.

Rahman, S., Brust, F., 1992a. An estimation method for evaluating energy release rates of circumferential through-wall cracked pipe welds. Eng. Fract. Mech. 43 (3), 417–430.

Rahman, S., Brust, F., November 1992. Elastic-plastic fracture of circumferential through-wall cracked pipe welds subject to bending. J. Press. Vessel Technol. 114 (4), 410–416.

Rahman, S., Wilkowski, G., Ghadiali, N., July 1993. Pipe fracture evaluations for leak-rate detection: probabilistic models. In: Garuch, Y.S. (Ed.) Proceedings of the ASME Pressure Vessels and Piping Conference, PVP-Vol. 266, Creep, Fatigue Evaluation, and Leak-Before-Break Assessment, Denver, Colorado, pp. 255–267.

Rahman, S., Wilkowski, G., Ghadiali, N., July 1993b. Pipe Fracture Evaluations for Leak-Rate Detection: Applications to BWR and PWR Piping. In: Garuch, Y.S. (Ed.) Proceedings of the ASME Pressure Vessels and Piping Division Conference, PVP-Vol. 266, Creep, Fatigue Evaluation, and Leak-Before-Break Assessment, Denver, Colorado, pp. 269–286.

Rahman, S., Brust, F., Ghadiali, N., Choi, Y.H., Krishnaswamy, P., Moberg, F., Brickstad, B., Wilkowski, G., April 1995. Refinement and Evaluation of Crack-Opening-Area Analyses for Circumferential Through-Wall Cracks in Pipes, NUREG/CR-6300. U.S. Nuclear Regulatory Commission, Washington, DC.

Rahman, S., Ghadiali, N., Paul, D., Wilkowski, G., April 1995. Probabilistic Pipe Fracture Evaluations for Leak-Rate-Detection Applications, NUREG/CR-6004. U.S. Nuclear Regulatory Commission, Washington, DC.

Rahman, S., Wilkowski, G., Brust, F., 1996. Fracture analysis of full-scale pipe experiments on stainless steel flux welds. Nucl. Eng. Des. 160, 77–96.

Rahman, S., Brust, F.W., Ghadiali, N., Wilkowski, G., 1998a. Crack-opening-area analyses for circumferential through-wall cracks in pipes — part I: analytical models. Int. J. Press. Vessels Pip. 75, 357–373.

Rahman, S., Brust, F.W., Ghadiali, N., Wilkowski, G., 1998b. Crack-opening-area analyses for circumferential through-wall cracks in pipes — part II: model validations. Int. J. Press. Vessels Pip. 75, 375–396.

Shih, C.F., Hutchinson, J.W., June 1986. Combined loading of a fully plastic ligament ahead of an edge crack. J. Appl. Mech. 53, 271–277.

Shih, C.F., 1985. J-dominance under plane strain fully plastic conditions: the edge crack panel subject to combined tension and bending. Int. J. Fract. 29, 73–84.

Sönnerlind, H., Kaiser, S., 1986. The J-integral for a SEN specimen under nonproportionally applied bending and tension. Eng. Fract. Mech. 24 (5), 637–646.

Wilkowski, G.M. et al., 1991–1995. Short Cracks in Piping and Piping Program, NUREG/CR-4599, Vols. 1–4, Nos. 1–2. U.S. Nuclear Regulatory Commission, Washington, DC.

Wilkowski, G., Rahman, S., Paul, D., Ghadiali, N., July 1993. Pipe Fracture Evaluations for Leak-Rate Detection: Deterministic Models. Proceedings of the ASME Pressure Vessels and Piping Conference, PVP-Vol. 266, Creep, Fatigue Evaluation, and Leak-Before-Break Assessment, Denver, Colorado, pp. 243–254.